IRAM

300, rue de la Piscine
38406 Saint-Martin-d'Hères (France)
Fax: (33/0) 476 42 54 69

Registration n°: **P300438**
Date: **15-SEP-2016**

PROPOSAL FOR THE 30M TELESCOPE

Title: CO redshift search for bright NIKA distant lensed galaxy candidates

PIs: Rémi Adam (FR), Alexandre Beelen (FR)
CoIs: H. Aussel (FR), Christophe Benoist (FR), Matthieu Bethermin (EU), Frederic Boone (FR), Alberto Cappi (FR), Gianluca Castignani (FR), Barbara Comis (FR), Francois-Xavier Desert (FR), Chiara Ferrari (FR), Oliver Hahn (FR), Guilaine Lagache (FR), Juan Macias-Perez (FR), Gerardo Martinez-Aviles (FR), Sophie Maurogordato (FR), Frédéric Mayet (FR), Laurence Perotto (FR), Nicolas Ponthieu (FR), Marina Ricci (FR), Florian Ruppin (FR)

Proposal category: Standard
Scientific category: Sub-mm Galaxies (SMG), Gravitational lenses, Galaxy structure & evolution, Galaxy Clusters

Total requested time: 21.3 (Emir)

Abstract:
High redshift dusty star forming galaxies play a fundamental role in galaxy formation and evolution. In the quest for probing these distant objects, galaxy clusters can serve as giant telescopes, thanks to the lensing magnification they produce, to observe galaxies that would be inaccessible otherwise. We propose to use EMIR to perform the CO redshift search of two lensed dusty star forming galaxy (DSFG) candidates amplified by PSZ1 G045.85+57.71, a cluster observed with NIKA+IRAM30m. This project will allow us to obtain a detailed view on the physics of DSFGs at high redshift. We will use EMIR at the IRAM 30m telescope, primarily in the E0 band, for a total of 21.3 hours. A companion proposal was also submitted to perform the follow-up of four fainter lensed galaxy candidates, from the same initial sample, with NOEMA.

Proposal history:
We have conducted Sunyaev-Zel'dovich (SZ) observations with the NIKA camera at the IRAM 30m telescope toward 6 clusters of galaxies in order to study the hot gas distribution in high redshift clusters and to prepare the NIKA2 SZ guaranteed time large program. Our primary goal, the mapping of the SZ effect at 150 GHz, was very successful and in addition our data have allowed us to detect sub-millimeter galaxies (in particular at 260 GHz), which are excellent high redshift lensed DSFG candidates. We therefore propose to follow-up a subset of these sources with EMIR.

Sources:

Id	Epoch	RA	DEC	z (redshift)
PSZ1G045S11	J2000	15:18:23.673	29:28:36.330	4.6
PSZ1G045S12	J2000	15:18:22.532	29:28:59.280	3.6

Emir technical sheet:
Time: 21.30
Frontend/Backend setups:

Setup	Band	Species/Transition	Frequency	Receiver band	T_A^*	Rms	ΔV	Backends
1	E0 (3mm)	CO	90.0	unspecified	3.15	0.63	80.0	FTS200
1	E0 (3mm)	CO	90.0	unspecified	2.55	0.51	80.0	FTS200

Observing parameters:

Setup	Observing mode	Size X	Size Y	Switch mode	PWV	Time	Repetition	Remark
1	Track			WSw	4	2.6	3	
1	Track			WSw	4	3.5	3	

Number of receiver tunings: 6

CO redshift search for bright NIKA distant lensed galaxy candidates

P.I.: Rémi Adam & Alexandre Beelen

1 Scientific context

Introduction Mapping the cosmic star formation history is one of the main topics of modern cosmology, on which rapid progress has been made in the last 20 years. We now know that star formation rate (SFR) density peaked approximately 3.5 Gyr after the Big Bang (Madau & Dickinson 2014) and declined exponentially at later times, with an e-folding timescale of 3.9 Gyr. At redshift $0.5 < z < 3$, **dusty star forming galaxies** (DSFGs) are dominating the history of cosmic star formation (e.g., Dole et al. 2006; Burgarella et al. 2013). At higher z, we are still lacking constraints on the contribution of dusty galaxy to the star formation density. Since optical/near-infrared observations select low dust content galaxies, observations in the (sub-)millimeter range are mandatory to target these DSFGs.

Despite the growing number of detected DSFGs at high-z, the detailed picture of the ongoing physical processes, which control star formation in these systems (e.g., environment, merger induced starburst, accretion of cold gas, feedback processes), is still subject to many open questions (Casey et al. 2014). This is in part due to **selection effects** induced by the dust obscuration of optical light that affects the corresponding surveys, or because (sub-)millimeter wide surveys mostly capture the bright end of the luminosity function of the underlying DSFG population.

Clusters as giant telescopes to probe distant galaxies The quest for high-z DSFGs has been extensively addressed using large (sub-)millimeter surveys such as H-ATLAS (Eales et al. 2010) or SCUBA-2 CLS (Geach et al. 2016), but they generally pick-up very luminous DSFGs that are not necessarily representative of the underlying population. A way to **access more typical DSFGs is to use the lensing magnification** induced by objects on the same line of sight, such as other galaxies or **galaxy clusters** (e.g., SPT results, Vieira et al. 2013). In large surveys, lensed DSFGs mostly arise from galaxy-galaxy lensing, but observations in the direction of clusters, aiming at capturing cluster-galaxy lensing, present several advantages: they allow for more accurate lensing modeling (necessary to correct observables from magnification); they provide an unobscured view of the background galaxies; the involved magnification factors are generally larger; and differential magnification effects are less important.

The search for bright high-z lensed DSFGs has been already used at sub-millimeter wavelength using, e.g., SCUBA (Knudsen et al. 2006) or the Herschel Lensing Survey (HLS, Egami et al. 2010). The discovered galaxies offer a possibility of **detailed multi-wavelength observations**, in which IRAM observatories have already played an important role (e.g., a $z = 5.2$ galaxy behind Abell 773, Combes et al. 2012).

The NIKA & NIKA2 cluster samples and proposed observations The New IRAM KIDs Arrays 2 (NIKA2) has been recently installed at the IRAM 30m telescope, offering simultaneous continuum observations at 150 and 260 GHz (Catalano et al. 2016). One of the **NIKA2** guaranteed time Large Programs will consist in the observation of about **50 clusters of galaxies** in the range $0.5 < z < 1$ (Comis et al. 2016). The primary goal of this program is to image the Sunyaev-Zel'dovich (SZ) signal from the clusters' hot gas at 150 GHz. However, at these redshifts, clusters also provide **optimal lenses for distant background galaxies**. Therefore, we anticipate the discovery of a large number of high-z lensed DSFGs at 260 GHz around the target clusters.

As a pilot project for the NIKA2 SZ large program, we have used the **prototype camera, NIKA**, to successfully map six massive clusters at $0.45 < z < 0.89$ (Adam et al. 2014, 2015, 2016a,b; Ruppin et al. 2016). We subsequently detected several DSFGs, of which many appear to be **excellent high-z lensed candidates**, in particular when combining NIKA and Herschel data. Our brightest candidate (lensed by CL J1226.9+3332 at $z = 0.89$, Adam et al. 2015) was also detected in HLS and has been confirmed spectroscopically as a z=2.4 lensed DSFG with EMIR (Egami priv. com.).

Here, we propose to perform the **CO redshift search** for the two brightest (and most reliable) **lensed DSFG candidates** selected from one of the NIKA cluster fields, **using EMIR**. As such galaxies are often too faint in optical, CO lines measurements are indeed the most efficient way to obtain spectroscopic redshifts, and in this context, EMIR is one of the most powerful instrument. Thanks to the strong magnification of our targets, we will be able to obtain a **rare view on typical DSFGs at high-z**. In addition, the observations will be used to optimize the scientific exploitation of NIKA2 and they will allow us to open up **synergies between NIKA2 and EMIR**. The cluster observations lead by our team at IRAM have been very fruitful, already resulting in 6 published/submitted papers, and this proposal is a natural continuation of this effort. A complementary companion proposal was also

submitted in order to observe 4 other fainter high-z DSFG candidates, from the same initial sample, with NOEMA (which are too faint for EMIR CO redshift search or have already been drawn). In particular, we aim at obtaining counterparts at other wavelength and study the connection between the optical and the sub-millimeter components (see also Table 1).

2 Technical justification

NIKA sources selection Four of the six NIKA clusters are part of the CLASH sample (Postman et al. 2012), for which a wealth of multi-wavelength data are publicly available, including deep HST, Spitzer, Herschel/PACS+SPIRE observations, and lensing models (e.g., Zitrin et al. 2015). The two remaining ones are **Planck clusters** for which HST (3 filters, in particular to obtain the cluster mass distribution via lensing measurement, P.I. Ebeling) and SPIRE data are available. For all clusters, we have additional X-ray and SZ (NIKA) data, which we routinely use to infer the total cluster mass distribution, allowing us to validate magnification estimates.

To **select lensed DSFG candidates**, we first built a source list by searching for compact objects in the highest magnification region around the clusters, in the **NIKA maps**. We then searched for Herschel counterparts, focusing primarily on the long wavelength bands, but also considering shorter wavelengths (figure 1). We extracted the NIKA and Herschel fluxes of these sources, and fit the SED with a modified blackbody spectrum, as illustrated in figure 2 (see Adam et al. 2016a, for details). A total of 17 candidates were thus found and one of the them is a known lensed DSFG at $z = 2.4$, recently measured with EMIR. This procedure provides a first photometric redshift estimate assuming a typical dust temperature of 35 ± 5 K and propagating (nearly gaussian) fitting uncertainties. Then, we use our best fit SED together with scaling relations between the infrared (IR) luminosity and the CO line intensity (Greve et al. 2014) to compute the expected CO(3-2) and CO(4-3) signal in EMIR E0 band. These lines are the most likely to be observed according to our redshift estimates (Carilli & Walter 2013), but the estimates remains comparable for other J lines. The source list and their main properties are given in Table 1. The two brightest candidates (in terms of CO line flux) with sufficiently well constrained SED (i.e., with the most accurate flux predictions), excluding SMG01 (already observed with EMIR), are SMG11 and SMG12 in the **field of PSZ1G045.85+57.71**. We therefore propose to observe these **two sources** (see figure 1).

Immediate objectives The proposed observations will allow us to fulfill the following immediate objectives. **1)** We will obtain **spectroscopic redshifts** for the two NIKA discovered distant DSFGs. This will provide a direct confirmation that our candidates are indeed high-z objects. **2)** The knowledge of the redshift will allow us to convert primary observables to physically relevant quantities, in order to characterize the **galaxy properties (SFR, IR luminosity, etc)**. **3)** We will estimate the amount of **molecular gas** of each galaxy and it will be compared to the **amount of dust** probed by continuum photometric data. **4)** Using the line profiles, we will search for **evidence of merging**, that may drive **starburst activity**. **5)** Finally, such observations will demonstrate the strong synergies between NIKA2 and EMIR observations.

Time estimates and configuration strategy Only three separate tuning are necessary to **cover the entire E0 band** from 73 to 117 GHz, with 16 GHz bandwidth. This corresponds to redshifts between 1.0 and 8.7 for CO lines between $J = 2 - 1$ and $7 - 6$, with only a small gap at $1.78 < z < 1.98$ that is very unlikely for our targets based on the photometric redshift estimates of Table 1. We propose to start the search in the lowest frequency band (using the tracked WSW observing mode) because of the better atmospheric conditions and the access to the lower J CO lines, the higher being possibly weaker. Once the first line is observed, we will search for a second one in the E1 band.

We consider the CO(3-2) and CO(4-3) lines because they are the most likely to be found in the E0 band at the expected redshift (4.6 and 3.6 for SMG11 and SMG12), but our estimates remain comparable for other J lines. For these two lines, we expect the flux to be, respectively, about 31 and 19 mJy for SMG11, and about 25 and 15 mJy for SMG12 (Table 1). We aim at a 5σ detection of the lines, which correspond for CO(3-2) and CO(4-3), respectively, to a rms of 1.05 and 0.63 mK for SMG11 and 0.84 and 0.51 mK for SMG12. We need a **resolution of 80 km/s** to ensure a good line sampling. Therefore, including 50% overhead for calibration, assuming a typical elevation of 50 degrees and average winter conditions (4.0 mm of pwv, Tsys 122.8 K[Ta*] mean per pixel), we require 2.6 hours and 3.5 hours of telescope time per tuning for SMG11 and SMG12 respectively, according to the EMIR time estimator. We allow 3 tunings in order to cover the full E0 band, and we add 30 min per tuning. Therefore, the total telescope time required to search for CO lines toward SMG11 and SMG12 are **9.3 hours and 12 hours, i.e., a total of 21.3 hours**. Finally, the two sources are observable $\sim$ 10 hours per day during the winter semester.

3 Supporting material

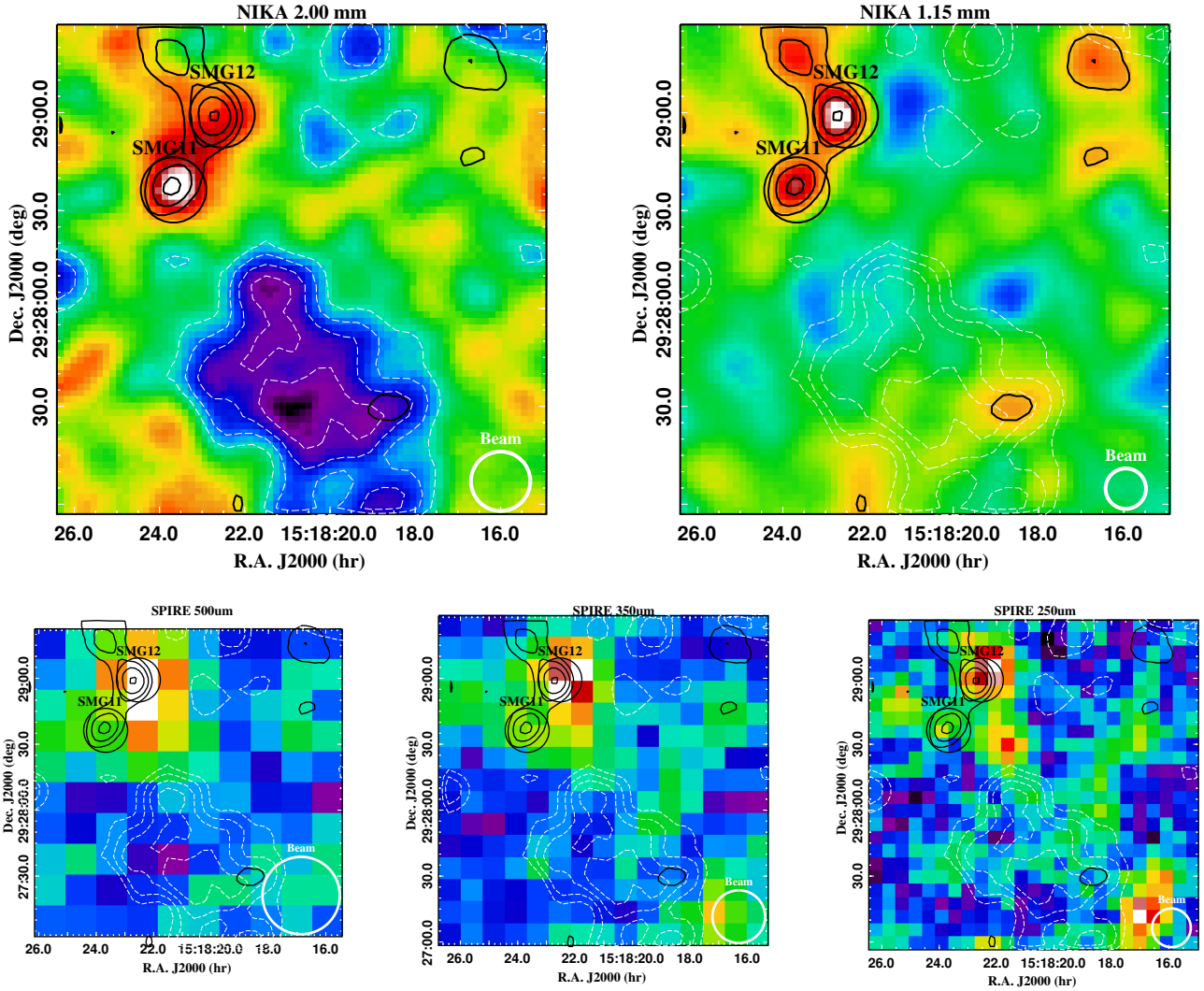

Figure 1: Millimeter (top) and sub-millimeter (bottom) maps toward PSZ1 G045.9+57.7. From top to bottom and left to right, the channels are NIKA 2.00 and 1.15 mm, and SPIRE 500, 350 and 250 μm. Black contours are reproduced from the 1.15 mm map to highlight the two bright DSFG candidates. The two candidates, labeled on the figure, are also identified by black circles. The elongated negative signal at 2.00 mm is due to SZ signal (Ruppin et al. 2016) and the white dashed contours are reproduced from this map to highlight the cluster mass distribution location. The white circles on the bottom right of each map provide the beam FWHM of each channel.

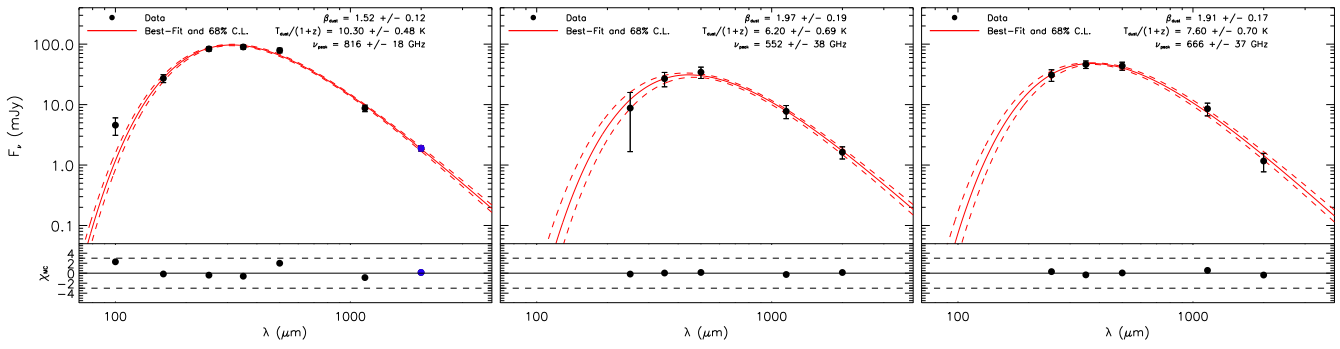

Figure 2: NIKA+Herschel SED and their modified black-body fit constraint. The blue point indicates possible contamination from SZ signal. **Left:** SMG01 (lensed by CL J1226.9+3332) – bright lensed DSFG with confirmed redshift at $z = 2.4$ from EMIR observations. Our redshift estimates gives $\hat{z} = 2.4 \pm 0.5$ for this source. This SED is provided as a reference for comparison. **Middle and right:** SMG11 and SMG12, respectively (lensed by PSZ1 G045.85+57.71) – high redshift candidates with $> 3\sigma$ NIKA detection in the two bands. Our redshift estimates gives $\hat{z} = 4.6 \pm 1.0$ and $\hat{z} = 3.6 \pm 0.8$ for SMG11 and SMG12, respectively. See also Figure 1.

Table 1: Summary of the properties of the lensed DSFG candidates. The 2 sources selected for the proposed observations are in bold face. The four sources proposed for NOEMA observations, in order to complement this proposal, are marked by †. Note that the physical quantities are not corrected for magnification to provide the direct observables. The CO line fluxes assume that the line widths are 400 km/s.

Source	R.A. (degree)	Dec. (degree)	1.15 mm flux (mJy)	2.00 mm flux (mJy)	SED peak (GHz)	$\beta_{\rm dust}$ (—)	$T_{\rm eff,dust}$ (K)	$\hat{z}_{\rm phot}$ (—)	$\hat{L}_{\rm IR}$ (10^{12} $L_\odot$)	$\hat{\rm SFR}$ ($M_\odot$ / yr)	$\hat{F}_{\rm CO(3-2)}$ (mJy)	$\hat{F}_{\rm CO(4-3)}$ (mJy)
RXJ1347.5-1145	— no strong candidate —											
CLJ1226.9+3332 SMG01†	186.74940	33.543114	8.7 ± 1.1	1.9 ± 0.2*	816 ± 18	1.52 ± 0.12	10.3 ± 0.5	2.4 ± 0.5	48.0	8202.0	18.7	11.8
CLJ1226.9+3332 SMG02†	186.75814	33.549083	3.1 ± 1.1	0.9 ± 0.3*	609 ± 66	2.05 ± 0.19	6.7 ± 1.0	4.2 ± 1.1	45.1	7706.3	16.5	10.4
MACSJ1423.8+2404 SMG03	215.94946	24.070625	8.6 ± 2.5	−0.4 ± 0.5**	911 ± 88	0.89 ± 0.20	14.0 ± 1.2	1.5 ± 0.4	3.7	641.2	1.8	1.4
MACSJ1423.8+2404 SMG04	215.93582	24.054733	4.6 ± 2.7	−0.3 ± 0.6	608 ± 792	2.17 ± 0.20	6.5 ± 10.0	4.4 ± 8.2	32.0	5480.4	11.7	7.6
MACSJ1423.8+2404 SMG05	215.94742	24.080956	4.2 ± 2.4	−0.8 ± 0.5**	751 ± 142	1.00 ± 0.19	11.1 ± 1.8	2.2 ± 0.7	5.7	971.5	2.3	1.7
MACSJ1423.8+2404 SMG06	215.97167	24.062847	7.6 ± 2.7	0.8 ± 0.6	359 ± 1530	2.05 ± 0.20	4.0 ± 18.9	7.8 ± 42.2	61.2	10472.3	25.7	15.8
MACSJ0717.5+3745 SMG07†	109.37740	37.745272	2.5 ± 0.7	0.6 ± 0.2*	424 ± 103	1.86 ± 0.19	4.9 ± 1.4	6.1 ± 2.3	25.9	4431.6	10.1	6.6
MACSJ0717.5+3745 SMG08	109.38925	37.734656	1.5 ± 0.7	−0.1 ± 0.2*	731 ± 1615	2.10 ± 0.20	8.0 ± 20.0	3.4 ± 11.1	11.8	2014.6	4.3	3.0
MACSJ0717.5+3745 SMG09†	109.39919	37.759447	1.7 ± 0.7	0.2 ± 0.2*	653 ± 150	2.38 ± 0.20	6.7 ± 2.0	4.2 ± 1.7	27.0	4610.0	9.9	6.5
MACSJ0717.5+3745 SMG10	109.35268	37.726572	1.4 ± 0.9	0.1 ± 0.2	865 ± 112	2.29 ± 0.19	9.0 ± 1.5	2.9 ± 0.9	18.8	3211.5	7.0	4.7
PSZ1G045.85+57.71 SMG11	229.59864	29.476758	7.7 ± 1.9	1.6 ± 0.4	552 ± 38	1.97 ± 0.19	6.2 ± 0.7	4.6 ± 1.0	84.2	14392.5	31.0	18.7
PSZ1G045.85+57.71 SMG12	229.59388	29.483133	8.5 ± 2.0	1.2 ± 0.4	666 ± 37	1.91 ± 0.17	7.6 ± 0.7	3.6 ± 0.8	67.9	11615.2	24.8	15.2
PSZ1G045.85+57.71 SMG13	229.57727	29.458097	4.5 ± 1.7	−0.8 ± 0.3**	389 ± 1570	2.06 ± 0.20	4.3 ± 19.3	7.2 ± 36.7	57.6	9854.6	23.4	14.5
PSZ1G045.85+57.71 SMG14	229.59208	29.447528	3.4 ± 1.7	0.3 ± 0.3*	801 ± 1506	0.92 ± 0.20	12.2 ± 18.8	1.9 ± 4.5	3.2	545.1	1.4	1.1
PSZ1G046.13+30.75 SMG15	259.28271	24.041972	3.5 ± 3.0	1.2 ± 0.5	635 ± 811	1.05 ± 0.21	9.2 ± 10.3	2.8 ± 4.2	11.6	1975.9	4.3	3.0
PSZ1G046.13+30.75 SMG16	259.26292	24.062750	−1.2 ± 2.4	1.0 ± 0.4*	762 ± 333	1.07 ± 0.20	11.0 ± 4.3	2.2 ± 1.3	7.7	1321.8	3.1	2.2
PSZ1G046.13+30.75 SMG17	259.28542	24.074583	0.0 ± 2.3	1.1 ± 0.4*	716 ± 860	0.92 ± 0.21	10.9 ± 10.7	2.2 ± 3.2	6.0	1024.2	2.4	1.8

Notes. * Possibly contaminated by SZ signal. ** Very likely to be contaminated by SZ signal.

References

R. Adam, B. Comis, J. F. Macías-Pérez, et al. (2014), A&A, 569, A66, ArXiv:1310.6237
R. Adam, B. Comis, J. F. Macías-Pérez, et al. (2015), A&A, 576, A12, ArXiv:1410.2808
R. Adam, B. Comis, I. Bartalucci, et al. (2016), A&A, 586, A122, ArXiv:1510.06674
R. Adam, I. Bartalucci, G. W. Pratt, et al. (2016), A&A, submitted, ArXiv:1606.07721
D. Burgarella, V. Buat, C. Gruppioni, et al. (2013), A&A, 554, A70, ArXiv:1304.7000
C.-M. Casey, D. Narayanan, & A. Cooray (2014), Phys. Rep., 541, 45, ArXiv:1402.1456
C. L. Carilli & F. Walter 2013, ARAA, 51, 105, ArXiv:1301.0371
A. Catalano, R. Adam, P. Ade, et al. (2016), ArXiv:1605.08628
F. Combes, M. Rex, T. D. Rawle, et al. (2012), A&A, 538, L4, ArXiv:1201.2908
B. Comis, R. Adam, P. Ade, et al. (2016), Moriond Proceeding, ArXiv:1605.09549
H. Dole, G. Lagache, J.-L. Puget, et al. (2006), A&A, 451, 417, ArXiv:0603208
J. E. Geach, J. S. Dunlop, M. Halpern et al. (2016), MNRAS, submitted, ArXiv:1607.03904
S. Eales, L. Dunne, D. Clements, et al. (2010), PASP, 122, 499, ArXiv:0910.4279
E. Egami, M. Rex, T. D.. Rawle, et al. (2010), A&A, 518, L12, ArXiv:1005.3820
E. Egami, private communication
T. R. Greve, I. Leonidaki, E. M. Xilouris, et al. 2014, ApJ, 794, 142, ArXiv:1407.4400
K. K. Knudsen, V. E. Barnard, P. P. van der Werf, et al. 2006, MNRAS, 368, 487, ArXiv:0602131
P. Madau & M. Dickinson 2014, A&ARA, 52, 415, ArXiv:1403.0007
M. Postman, D. Coe, N. Benítez, et al. 2012, ApJS, 199, 25, ArXiv:1106.3328
F. Ruppin, R. Adam, B. Comis, et al. 2016, A&A, submitted, ArXiv:1607.07679
J. D. Vieira, D. P. Marrone, S. C. Chapman, et al. 2013, Nature, 495, 344, ArXiv:1303.2723
A. Zitrin, A. Fabris, J. Merten, et al. 2015, ApJ, 801, 44, ArXiv:1411.1414